

EMPIRICAL VULNERABILITY ASSESSMENT FOR LOW RISE RC, TIMBER AND MASONRY ICELANDIC BUILDINGS

Bjarni BESSAON¹, Ioanna IOANNOU², Ioannis KOSMIDIS³, Jón Örvar BJARNASON⁴,
Tiziana ROSSETTO⁵

ABSTRACT

The South Iceland Seismic Zone (SISZ) is about a 70-km long belt lying in the east-west direction and 10-15 km wide in the north-south direction. Approximately 20 earthquakes with magnitudes in the range of 6 to 7 have occurred in this zone since 1700. These events tend to occur in sequences and therefore structures may be exposed to strong ground motion from more than one event within a few days. The SISZ crosses the largest agricultural region in Iceland with small towns, farms and all the infrastructure assets of a modern society. On 17 and 21 of June, 2000, two Mw6.5 earthquakes struck the SISZ. Both were shallow strike-slip quakes with parallel fault ruptures and with an approximately 16 km fault-to-fault distance. They affected nearly 5000 low-rise residential buildings. All buildings in Iceland are registered in a detailed official inventory. Furthermore, all buildings are covered by compulsory catastrophic insurance and therefore, after the earthquakes, damage and repair costs for every damaged building were assessed for insurance purposes. The collected loss data merged with the real estate register data were used in the present study to assess a vulnerability model based on beta regression. Critical in the development of the methodology were the determination of which buildings sustained damage due to one or two events, secondly the problem of substantial variability in the loss data, and finally uneven spatial distribution of the buildings due to villages on one hand and single farms on the other hand.

Keywords: Vulnerability mode; Fragility curves; Loss data; RC buildings; Timber buildings.

1. INTRODUCTION

Seismic hazard is high in Iceland and comparable to what is experienced in South Europe. The population has historically been low and the inhabited areas sparsely settled. As a result, the consequences of major earthquakes have been low on an international scale and have received little attention. In recent times, villages have been established in locations which used to be rural, and a greater number of structures and infrastructure have been built, creating a larger exposure to losses from natural hazards. The origin of the most destructive earthquakes is found in two complex fracture zones (Einarsson 1991). The one is in the south and named the South Iceland Seismic Zone (SISZ) and the other is in the north and identified as the Tjörnes Fracture Zone (TFZ), where the main activity is offshore (Figure 1). In this paper the focus is on the SISZ. Since the year 1700 there have been 20 earthquakes of magnitude six or greater in the SISZ and three of them have occurred since 2000 (Halldórsson et al. 2013). These earthquakes are associated with a strike-slip motion at shallow depth

¹Professor, Faculty of Civil and Environmental Engineering, University of Iceland, Reykjavik, Iceland bb@hi.is

²Research Associate, EPICentre, Department of Civil, Environmental and Geomatic Engineering, University College London, UK, ioanna.ioannou@ucl.ac.uk

³Senior Lecturer, Department of Statistical Science, University College London, and The Alan Turing Institute, London, UK, i.kosmidis@ucl.ac.uk

⁴Senior Engineer, Iceland Catastrophe Insurance, Kópavogur, Iceland, jonorvar@vidlagatrygging.is

⁵Director and Professor, EPICentre, Department of Civil, Environmental and Geomatic Engineering, University College London, UK, t.rossetto@ucl.ac.uk

(5-10 km). The upper bound of historical earthquakes is estimated to be around 7.0. Larger earthquakes are not expected due to the fault mechanism, crust strength and crust thickness. Another important characteristic of the seismicity in the SISZ is that the major earthquakes tend to occur in sequences. One such sequence occurred in 1784 when two earthquakes of magnitudes M_S 7.1 and 6.7 struck in two days with approximately 25 km fault distances. In 1896 five earthquakes of magnitudes M_S 6.9, 6.7, 6.0, 6.5 and 6.0 struck in two weeks with a 50-km distance between the most western and most eastern faults (average fault distance 12.5 km) (Sigbjörnsson & Rupakhety 2014). More recently, two M_w 6.5 and 6.5 earthquakes with a 15-km fault distance struck on the 17th and 21st of June 2000 (Figure 1).

In Iceland, all buildings are registered in an official database which contains detailed information such as date of construction, number of floors, floor area, main building material, geographical location, type of use, replacement value, etc. Natural catastrophe insurance of all buildings is mandatory and is administrated by the Iceland Catastrophe Insurance (ICI). Therefore, after catastrophic events like large earthquakes, the repair cost for every damaged building is estimated by trained assessors in order to settle the individual insurance claims.

The two June 2000 earthquakes had epicentres and fault ruptures in the middle of the South Iceland lowland, which is the largest agricultural region in the country, surrounded with mountain areas in the west, north and east (Figure 2). These events caused a lot of building damage but fortunately no residential buildings collapsed and there were no fatalities or serious injuries. The insurance vulnerability surveys were carried out in the aftermath of the second event, and hence the areas affected by both earthquakes reflect losses accrued over the two events. The collected loss data have been merged with the real estate register and this has resulted in detailed and complete loss data for the whole affected region. Almost 5000 low-rise residential buildings were affected by these earthquakes ($PGA > 0.05g$).

Although the data are of high quality there are challenges to deal with when developing a statistical vulnerability model. The first challenge is that some of the affected buildings were exposed to intense ground motion from two destructive earthquakes and therefore may have experienced

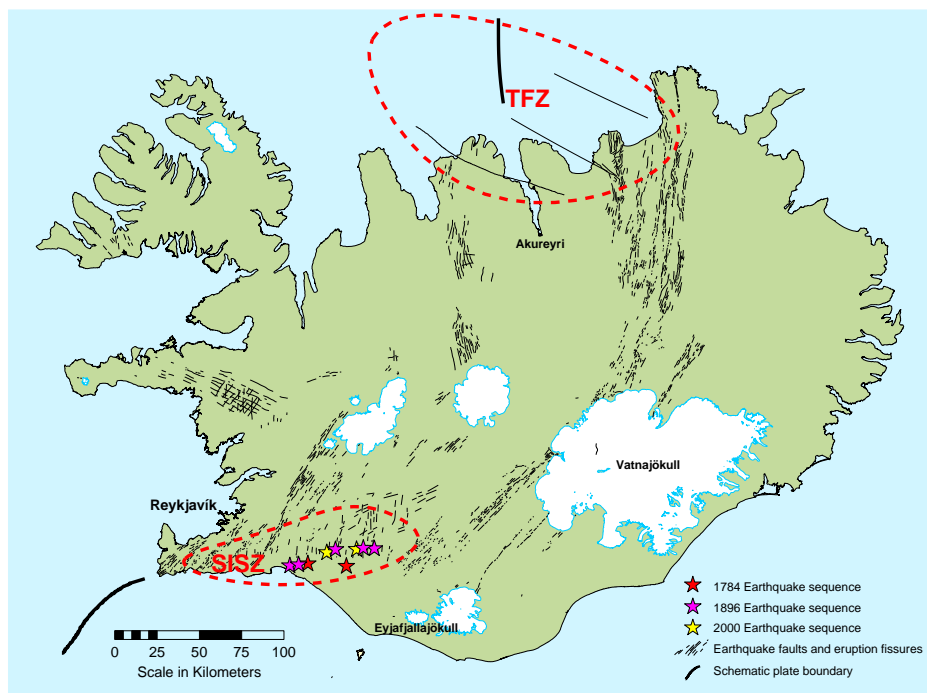


Figure 1. The South Iceland Seismic Zone (SISZ) and the Tjörnes Fracture Zone (TFZ). Locations of epicentres of the two 1784 earthquakes, the five 1896 earthquakes and the two June 2000 are shown with stars (The map is based on data from the Icelandic Institute of Natural History and National Land Survey of Iceland).

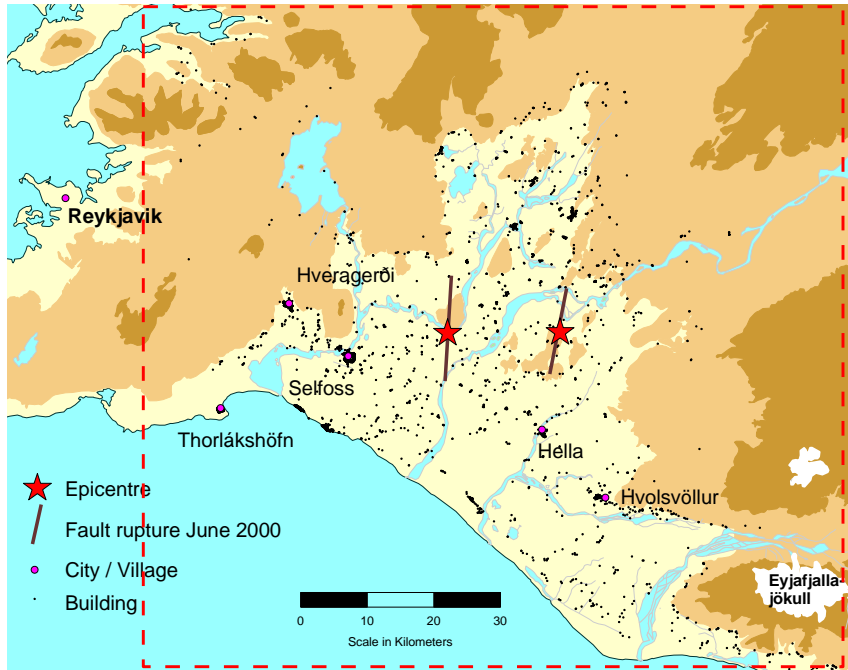


Figure 2. Epicentres and fault ruptures of the two June 2000 South Iceland Mw6.5 earthquakes. The residential buildings within the dotted red rectangle were used in the study. The largest village in the area, Selfoss, had 4500 inhabitants in 2000. (Map data from the National Land Survey of Iceland and Register Iceland).

accumulated losses. The second challenge is that the buildings are unevenly spatially distributed over the region. On one hand there are villages and other building clusters and on the other hand there are single farms. Finally, the third challenge is that there was substantial variability in the loss data for a given intensity level. A subset of the data, where all buildings located between the two faults were omitted, has been used to develop fragility curves (Bessason & Bjarnason 2016). This study on the other hand is based on more advanced methodology where beta regression and statistical tests were used to find the best fit model to the whole dataset. The new model is capable to deal with all the three mentioned challenges (Ioannou et al. 2017). The aim of this paper is to present the main characteristic of the loss data and some results based on the beta regression model. Vulnerability functions as well as fragility curves are given for the main building typologies for two cases, i.e. buildings affected by one event and buildings affected by two events.

2. GROUND MOTION AND DESCRIPTION OF LOSS DATA

2.1 *The South Iceland earthquakes of June 2000 and the intensity parameter*

Two earthquakes struck in the SISZ in June 2000 (Figure 2). The first Mw6.5 earthquake struck on June 17, 2000, at 15:41 (GMT). It was a right-lateral strike-slip quake, with fault striking in the north-south direction and had a focal depth of 6.3 km. Subsurface fault mapping based on the micro-earthquakes showed an approximately 12.5-km long and 10-km deep vertical fault rupture (Vogfjörd et al. 2013). The highest recorded Peak Ground Acceleration (PGA) was 0.64 g. The second earthquake, also of Mw6.5, struck on June 21, 2000, at 00:52, (GMT). It was as well a right-lateral strike-slip earthquake, with the fault striking in the north-south direction and with a focal depth of 5.3 km. Subsurface fault mapping based on the micro-earthquakes showed an approximately 16.5-km long and 7–9-km deep almost vertical fault rupture (Vogfjörd et al. 2013). The highest recorded PGA was 0.84 g (Thórarinnsson et al. 2002). Time histories and response spectra from these events can be found in the ISESD database (Ambraseys et al. 2002). The largest aftershock was $M_L 5.0$ and all the others were of a magnitude less than $M_L 4.5$ (Bessason & Kaynia 2002).

In vulnerability assessment, it is necessary to use an intensity measure that has good correlation with the observed damage. In the analytical vulnerability literature, most recent studies consider spectral acceleration or spectral displacement at representative structural periods to be the most effective intensity measures for vulnerability assessment (D' Ayala & Meslem 2013). Such measures have also been used in the empirical vulnerability literature. However, unless a spectral intensity measure is evaluated at for specific structural period value (e.g. $T = 0.2s$), the use of spectral values in empirical vulnerability studies introduces an as-yet unmodelled epistemic uncertainty, i.e. in the estimation of the structural period of the affected buildings. It is also well known that damage of structural elements as well as non-structural elements and household contents depends on a combination of high amplitude action effect and repeated stress reversals at significant amplitude (see for instance Park & Ang 1984). High frequency peak values of ground motion, especially PGA and low period spectral acceleration, can be observed in low magnitude earthquakes, but duration of significant intensive ground motion is more correlated with magnitude.

No site-specific ground motion prediction equations (GMPE) are available to predict duration of significant ground motion intensity in the SISZ. On the other hand, few GMPE models exist for PGA and the spectral ordinates which are based on Icelandic strong motion data. In the current study the affected buildings were low-rise, stiff and with low natural periods and therefore the ground motion intensity was expressed in terms of the PGA, which is representative of the short period part of a response spectrum. The GMPE of Rupakhety and Sigbjörnsson (2009) was adopted:

$$\log_{10}(PGA) = -1.038 + 0.387 \cdot M_w - 1.159 \cdot \log_{10} \left(\sqrt{H^2 + 2.6^2} \right) + 0.123 \cdot S + \varepsilon \cdot 0.287 \quad (\text{m/s}^2) \quad (1)$$

where H is the distance to surface trace of the fault in km, S is a site factor which takes the value 0 for rock sites and 1 for stiff soil sites. A geological map of South Iceland, which depicts locations and areas of sediments, was used to determine the soil conditions at each building site (Jóhannesson et al. 1992). The last term is an error/scatter term where ε is standard normal distributed, i.e. $\varepsilon \sim N(0,1)$. Following common practice, the PGA level at a given location was estimated as the median PGA from Equation 1, ignoring the error term. The adopted GMPE was based on using both the horizontal peak components from each station. Most of the strong motion recordings used in constructing Equation 1 were from Icelandic earthquakes but the database was also augmented by records from continental Europe and the Middle East. The main characteristic of the GMPE (Equation 1) is that it predicts a relatively high PGA in the near fault area whilst the attenuation with distance is more than generally found in a well-known GMPE of similar form. This higher attenuation with distance in Iceland compared to other seismic regions has been explained by the existence of young, fissured and low quality rock in the seismic source area that damps the propagating seismic waves faster than in more solid rock (Sigbjörnsson et al. 2009; Ólafsson 2013).

2.2 Property database and loss database

Based on the official property database approximately 85% of all apartments in Iceland are in reinforced concrete (RC) buildings, 12% in timber buildings and 3% in masonry buildings (Icelandic Property Registers, 2015). The composition of apartments in the affected area in the SISZ, however, is different from those numbers. The area consists mainly of agricultural land with many farms and few small villages and service centers. The vast majority of residential buildings are low-rise single-family buildings, but there are also two-family duplexes, town houses and apartment buildings (blocks). Buildings higher than 3 stories hardly exist. The present study was restricted to these low-rise residential buildings, which represent the overwhelming majority of the buildings in the studied area. The detailed property database gives the opportunity to classify the building stock with respect to different parameters, such as building material, age, and number of stories. Different classifications were tested but the conclusion was to distinguish between three typologies: RC buildings, timber buildings and masonry buildings. The great majority of residential buildings in Iceland have walls for resisting lateral seismic forces (Bessason et al. 2012). This is true for RC and timber as well as masonry buildings. The masonry buildings, mainly erected before 1980, were built of unreinforced

manufactured hollow pumice blocks in walls and tied together with rigid RC floors. The building stock is young and mostly built after 1950 (Bessason et al. 2014). None of the buildings were built before 1870. Seismic codes were implemented in 1976 in Iceland and caused an increase of reinforcement in RC buildings. All the losses in the aftermath of the two June 2000, South Iceland earthquakes, were estimated for each individual apartment instead of each building. In this study the original database was simplified by aggregating losses from all apartments within the same building. Here, “building” was defined by the street address. As an example, a building (block) with 12 apartments divided by three staircases, each with its own street address, was classified as three buildings. The loss data for each building were classified according to five sub-categories of structural and non-structural damage (Table 1). The non-structural damage does not include damage of loose household equipment like furniture, electronics (TVs, computers), etc. Previous studies of the subcategorized loss data from recent Icelandic earthquakes showed that non-structural loss dominated the overall loss in the June 2000 earthquakes (Bessason & Bjarnason 2016) as well as in the May 2008 Mw6.3 (Bessason et al. 2014). This study, however, concentrated on the total repair cost (i.e., the aggregated loss in all five sub-categories) normalized with the replacement value taken from the official property database:

$$Loss = \frac{\text{Estimated total repair cost}}{\text{Replacement value}} \quad (2)$$

The loss cannot be greater than 1 (100%) and in practice the expression “total damage” was assigned to residential buildings that suffered an estimated repair cost of more than 70% of their replacement value. In these cases, full replacement cost is paid to the owner. In this study, 100% loss was used whenever the owners received the full replacement cost despite the fact that the actual repair cost was estimated as lower. The derived vulnerability curves therefore incorporate local policy for insurance pay-out. According to ICI, the replacement value reported in the database is the same as the fire insurance value of a building, and is the depreciated replacement value plus the cost of removing the destroyed building. The depreciation is based on age, building material and general condition. On the other hand, the repair cost (loss) is in general not depreciated. To get an overview the data were classified for each building typology in five groups with different intensity defined by PGA bins (Figure 3). In all cases the maximum PGA from the two events was used, i.e. $PGA = \max(PGA_{EQ17June}, PGA_{EQ21June})$. For all the building typologies most of the affected buildings ($PGA > 0.05g$) were exposed to two first PGA bins (0.05-0.10g and 0.10-0.20g) (Figure 3a, 3b and 3c). This was both due to the fact that larger areas were included in the lower bins compared to the higher bins and, secondly, because the main villages were located in the lower PGA bins. At the lower two intensity bins most of buildings had no loss. At higher intensity more buildings were assigned loss but the scatter was quite wide and there were buildings with both no loss and total loss at the same intensity (Figure 3d, 3e and 3f). Figure 4a, 4b and 4c shows box plots for the three building typologies. The central mark indicates the median, and the bottom and top edges of the box indicate the 25th and 75th percentiles (p_{25} and p_{75}), respectively. The whiskers extend to the most extreme data points not considered outliers, defined as $p_{25} - (p_{75} - p_{25})$ and $p_{75} + (p_{75} - p_{25})$. The outliers are plotted individually using the '+' symbol. For the two lowest intensity bins and for all the three building typologies the medians p_{25} and p_{75} are at the same loss level (Loss=0.0). The number of outliers in all cases indicates the scatter in the data. Even at low intensity there are examples of “total loss” (Loss=1.0). The mean loss values are in all cases higher than the median (Figure 4d, 4e and 4f).

Table 1. Sub-categories of the loss data from the 2 June, 2000, South Iceland earthquakes.

Category	No.	Subcategory
Structural damage	1	Excavation, foundations and bottom slab.
	2	Interior and exterior supporting structure (walls, columns, beams, roofs).
Non-structural damage	3	Interior finishing work (partition walls, mortar, suspended ceilings, cladding).
	4	Interior fixtures, paintwork, flooring, wall tiles, windows, doors, etc.
	5	Plumbing (cold water, hot water and sewer pipes), radiators, electrical installations.

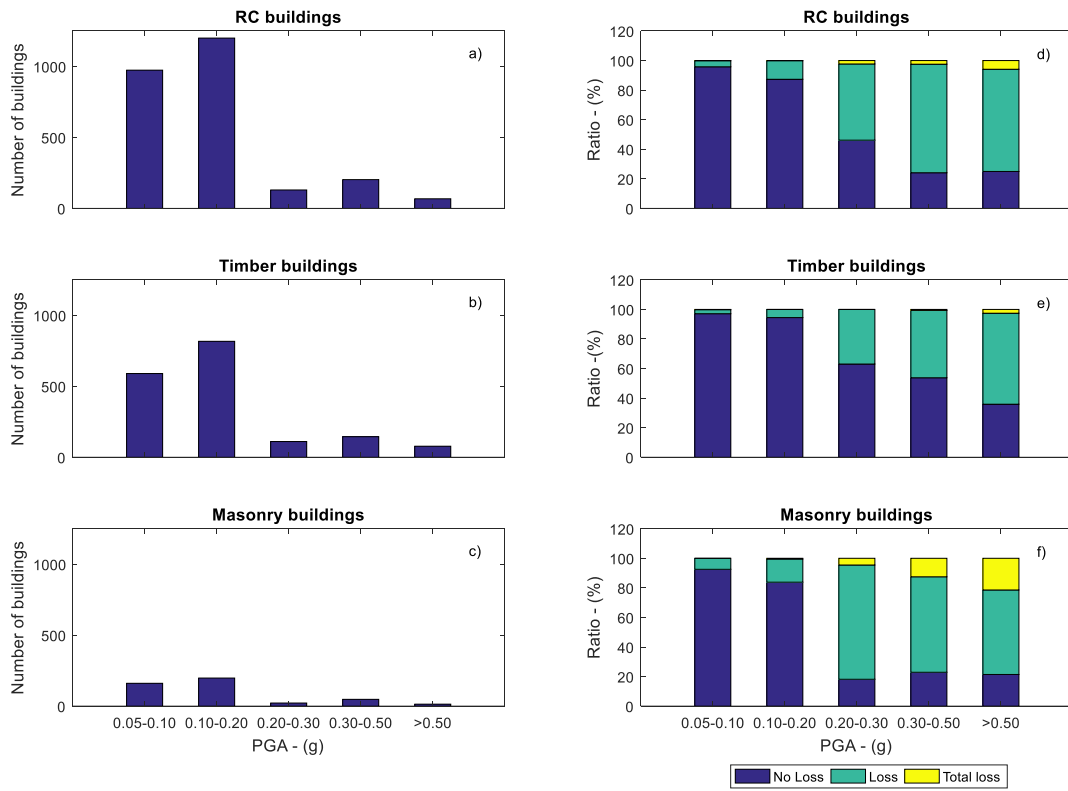


Figure 3. *Left bars*: Number of buildings for the three typologies as a function of acceleration bins. *Right bars*: Damage distribution between “No loss”, “Loss” and “Total Loss” as a function of acceleration bins.

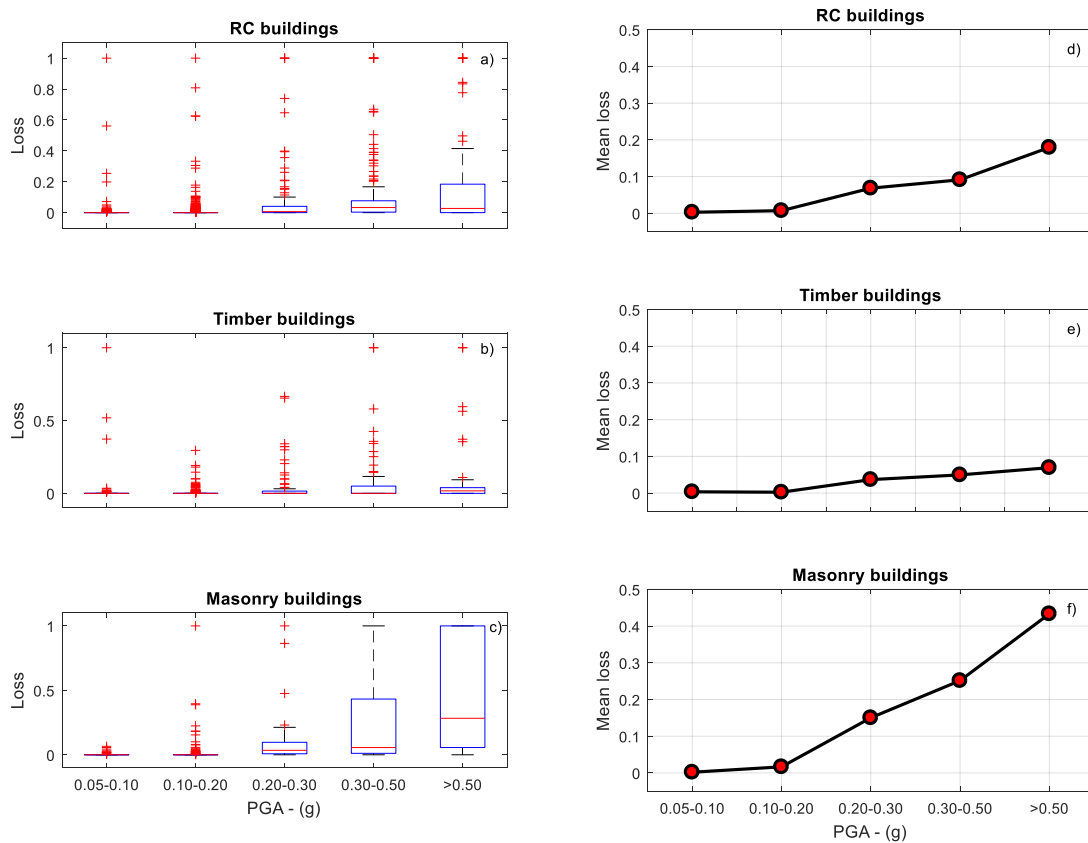


Figure 4. *Left graphs*: Box plots of loss for the three typologies for different acceleration bins. *Right graphs*: Mean loss for the three typologies for different acceleration bins (all data).

3. STATISTICAL MODEL

3.1 Proposed methodology

Initially the aim was to construct a statistical seismic vulnerability model for the Icelandic loss data based on the methodology developed by Rossetto et al. (2013, 2014). This was not straightforward, however, due to three main reasons: First, the wide scatter in the losses for the same intensity level (Figure 3 and 4); secondly, uneven spatial distribution of the buildings due to clusters in small towns and villages on one side and then well spatially distributed single buildings at farms on the other side (Figure 2 and 3); and third, many of the buildings had been affected by two earthquakes, i.e. an earthquake sequence, and may therefore have undergone accumulated damage (Figure 2). The two first points made it necessary to aggregate the data before fitting a statistical model and the third point requested some methodology to distinguish between buildings affected by one event and those affect by both events. The framework of the proposed methodology has four main steps (Figure 5).

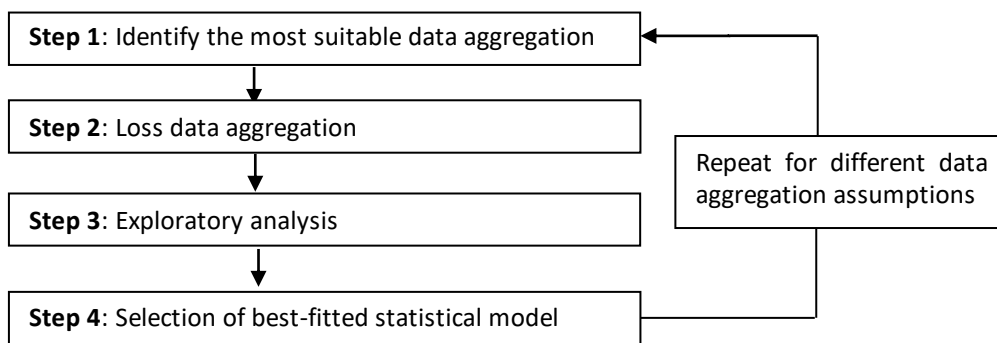


Figure 5. Proposed seismic vulnerability assessment methodology for sequence of earthquakes

According to the suggested methodology, the data were aggregated using an adaptive spatial grid in accordance with a number of assumptions. Then an exploratory analysis followed in order to identify the important explanatory variables. The outcome of the exploratory analysis was used to construct appropriate statistical models which were then fitted to the data. Goodness of fit tests were then employed to identify the model which best assessed the seismic vulnerability of an area affected by a sequence of events. These steps were repeated for different data aggregation assumptions. What follows outlines in more detail how the proposed methodology was fitted to the Icelandic loss data.

3.2 Loss data aggregation

The data aggregation was based on building location and relied on an adaptive spatial grid constructed as follows. The $\max PGA$ from the two events was estimated on an equi-spaced, dense grid of coordinates ($1 \text{ km} \times 1 \text{ km}$) within the affected area (i.e., 80 km in the east-west \times 100 km in the south-north direction). The PGA for each event and grid point was estimated from the GMPE expressed by Equation 1, accounting for the soil conditions. The spatial grid was then constructed by defining a partitioning of the available area into non-overlapping rectangles, where the standard deviation of the $\max PGA$ estimates within each rectangle does not exceed a pre-specified threshold ($threshold_{stdev}$). The construction of the partitioning was done recursively by partitioning the available area into 4 equi-area rectangles, and examining whether the observations in each rectangle satisfy the standard deviation threshold. If the standard deviation of the $\max PGA$ was below the preselected threshold, the partition process was stopped. The threshold was selected arbitrarily. In this study, three thresholds (i.e., 0.05 g , 0.10 g and 0.15 g) were tested. Overall, the smaller the $threshold_{stdev}$, the smaller the sample of buildings in each grid rectangle. It was found that a $threshold_{stdev}$ equal to 0.10 g provided a large sample size of grid rectangles with an adequate building aggregation in each grid rectangle (Figure 6). The grid rectangles are smaller in size for the areas close to the two faults and larger in the areas further away.

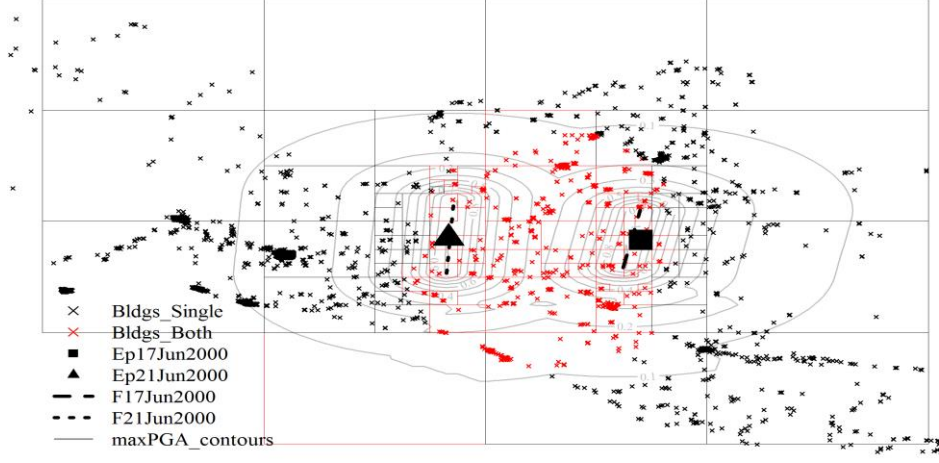


Figure 6. Locations of the residential buildings and maxPGA contours of the 17 and 21 June 2000 events. Adaptive grid rectangles are shown using $threshold_{stdv}=0.10g$. Buildings affected by both events are show by red marks and by black marks if affected by both events based on the criterion that $threshold_{minPGA}=0.10 g$.

3.3 Exploratory analysis

Having partitioned the affected area, values regarding the loss as well as a number of potentially statistically significant explanatory variables were determined from the aggregated data in each grid rectangle. After aggregation the loss was estimated as the ratio of the sum of the repair cost of the residential buildings in each rectangle located over the sum of their replacement cost:

$$loss_j = \frac{\sum_{i=1}^{N_j} repair\ cost_i}{\sum_{i=1}^{N_j} replacement\ cost_i}, \quad j = 1, 2, \dots, M \quad (3)$$

where N_j is the total number of buildings in a given rectangle j and M are the total number of rectangles.

A number of continuous and categorical explanatory variables were tested to find the best-fit statistical model. The continuous variables include the maxPGA for each grid rectangle which was estimated as the maximum of the mean PGA levels of the two events for the buildings in the examined rectangle. The categorical variable *Event* was used to express whether a grid square was affected by a single event or both events of the June 2000 sequence. The boundary between the area affected by a single event and both events was determined in this study as follows. The minimum PGA (minPGA) level from the two June earthquakes was estimated for each building. The value was compared to a pre-specified minPGA threshold ($threshold_{minPGA}$). If the minPGA level for a given building was above the threshold, the building was considered to have been affected by both events. Otherwise, the building was considered to have been affected by a single event, without distinguishing whether it was the 17 June or the 21 June earthquake. The $threshold_{minPGA}$ is an arbitrary value. For the needs of this study, the three values 0.05g, 0.10g and 0.15g were considered. The study indicated that a $threshold_{minPGA}$ equal to 0.10 g provided a large enough intensity to expect cumulative damage from two events. The area affected by both events based on this value includes the faults from both events (Figure 6). Three different ways to define building characteristics were tested by categorical variables, i.e. according to the main construction material (*RC, timber, masonry*), construction age (*pre-1980, post-1980*), and a combination of construction material and age (for more details, see Ioannou et al. 2018). The study showed that using construction material gave the best result. Finally, the continuous variable area of each grid rectangle (in km²) was tested and it did not improve the results. The Akaike

Information Criterion (AIC) (Akaike, 2011) was used to find the model that best fitted the data.

3.4 Selection of statistical model

Having identified the potentially important explanatory variables, multiple statistical models were tested using the two thresholds: $threshold_{stdv} = 0.10g$ and $threshold_{minPGA} = 0.10g$. Given that loss is a continuous variable bounded in the unit interval of (0,1), it was assumed that the loss followed a beta distribution, which has probability density function, expected value and variance, respectively:

$$\begin{aligned}
 f(l; \mu, \varphi) &= \frac{\Gamma(\varphi)}{\Gamma(\mu\varphi)\Gamma(1-\mu)\varphi} l^{\mu\varphi-1} (1-l)^{(1-\mu)\varphi-1} & 0 < l < 1 \\
 E[L; \mu, \varphi] &= \mu & 0 < \mu < 1 \\
 \text{Var}[L; \mu, \varphi] &= \frac{\mu(1-\mu)}{1+\varphi} & \varphi > 0
 \end{aligned} \tag{4}$$

In Equation 4, μ is the mean value and φ is the precision. A beta regression model links μ and possibly φ with a systematic component that is a function of a vector of explanatory variables. The mean value, μ , is related to the explanatory variables through a link function, $g_1(\cdot)$:

$$\mu = g_1^{-1}(\eta_1) \tag{5}$$

where η_1 is a function of the explanatory variables. In this study, the logit link function was adopted:

$$g_1(\mu) = \text{logit}(\mu) = \log\left(\frac{\mu}{1-\mu}\right) \tag{6}$$

Similarly, φ can also be considered as a constant intercept or a function of the explanatory variables, η_2 , through a link function, g_2 :

$$\varphi = g_2^{-1}(\eta_2) \tag{7}$$

where η_2 is determined by the plot of residuals against η_1 . If the residuals appear to be randomly distributed the use of a constant precision is adequate. The presence of heteroskedasticity, the increase or decrease of the scatter of the residuals with the increase in η_1 , indicates the need for a more complex expression of the precision which account for explanatory variables. In this study, the link function of the precision is expressed in the form:

$$g_2(\varphi) = \log(\varphi) \tag{8}$$

Having determined the main properties of the statistical model, η_1 and η_2 need to be expressed as functions of the explanatory variables. Based on the above explanatory analysis, the working form of η_1 was set to include both the ground motion intensity ('maxPGA') as well as the variable which captures whether the area has been affected by a single or both events ('Event'). It should be noted that this study deviates from other studies in the incorporation of the building characteristics in the statistical model. So far, empirical vulnerability curves have been developed for given building classes. In contrast, this study concentrated on estimating the seismic loss in a given rectangle grid which had a certain distribution of building characteristics, e.g., 70% RC, 20% timber and 10% masonry. The best model of the total of eight models tested was found based on the AIC and likelihood-ratio test (for more detail, see Ioannou et al. 2018):

$$\eta_1 = \theta_0 + \theta_1 \times \ln(\max PGA) + \theta_2 \times Event + \theta_3 \times Masonry + \theta_4 \times Timber + \theta_5 \times RC \quad (9)$$

$$\eta_2 = \theta_0' + \theta_1' \times Event$$

It should be noted that, in Equation 9, the explanatory variables associated with the percentage distribution of the building characteristics (*RC*, *timber*, *masonry*) are not independent as their sum is constant and must always be equal to 100% for each grid rectangle. This violates one of the main assumptions on which a meaningful regression is based, i.e. the need for the explanatory variables to be independent. To address this issue, the constant-sum explanatory variables, x_i , were transformed through an isometric log-ratio transformation (Neocleous 2011). The transformed explanatory variables can be written as:

$$z_i = \sqrt{\frac{D-i}{D-i+1}} \ln \left(\frac{x_i}{\sqrt[D-i]{\prod_{j=i+1}^D x_j}} \right), \quad i = 1, \dots, D-1 \quad (10)$$

where D is the total number of constant-sum explanatory variables, i.e. $D = 3$ for the classification of building according to building material, x_1 , x_2 and x_3 refer to percentages of masonry, timber, and RC buildings, respectively, in a given rectangle, i.e. $x_1 + x_2 + x_3 = 100\%$. Ideally, all building classes of a given scheme should be present in a grid rectangle in order for the transformation in Equation 10 to be meaningful. This, however, is an unrealistic expectation for the available database, where it is not uncommon to have grid rectangles where at least one building class is not represented. The aggregation of the buildings according to a single structural characteristic (i.e., only material or only age) instead of two reduces the number of missing classes in the grid rectangles but does not eliminate them. Unrepresented classes in a given rectangle grid were considered equal to 0.001 in order to make the transformation possible (Neocleous 2011). The working form of η_1 after the transformation of the constant-sum explanatory variables is depicted in Equation 11. The model for η_2 is unchanged.

$$\eta_1 = \theta_0 + \theta_1 * \ln(\max PGA) + \theta_2 * Event + \theta_3 * z_{Mat,1} + \theta_4 * z_{Mat,2} \quad (11)$$

$$\eta_2 = \theta_0' + \theta_1' \times Event$$

4. RESULTS AND DISCUSSION

The regression coefficients for the statistical model given by Equation 11 are depicted in Table 2. The model can be used to obtain different information. In Figure 7a, 7b and 7c, the mean loss curves are shown for rectangles with only RC buildings, only timber buildings and only masonry buildings as a function of PGA. Two scenarios are shown, i.e. when the buildings were affected by a single event and when they were affected by two events. For comparison the mean values from the raw data, i.e. before aggregation covering all buildings of the same typology are shown for different acceleration bins (0.05-0.10 g, 0.10-0.20 g, 0.20-0.30 g, 0.30-0.50 g, >0.50 g). The mean value of all maxPGA values, $\max(PGA_{17\text{June}}, PGA_{21\text{June}})$, for each building within the specified acceleration bin was used as the x-coordinate. Beforehand it would have been expected to see these data points lying between the ‘‘Single’’ and ‘‘Both’’ curves, but this was not always true. One reason is that the statistical model is based on aggregated data and another reason is that curves are forced to follow the functional form given by Equation 11. From the statistical model it is also possible to construct fragility curves both for buildings affected by a single event (Figure 7d, 7e and 7f) or both events (Figure 7g, 7h, and 7i). Four damage states were defined: DS0 – minor, loss less than 1% of replacement value; DS1– slight, 1-5% loss; DS2 – moderate, 5-20% loss; DS3 – substantial, 20-50% loss. In all cases the probability of exceeding DS3 was less than 15%, except for masonry buildings affected by both events.

Table 1: Regression coefficients for the model given by Equation 11.

	θ_0	θ_1	θ_2	θ_3	θ_4	θ'_0	θ'_1
Mean estimates	-2.24	0.45	1.35	0.14	-0.01	2.10	-1.37
Standard error	0.331	0.162	0.357	0.036	0.033	0.288	0.361

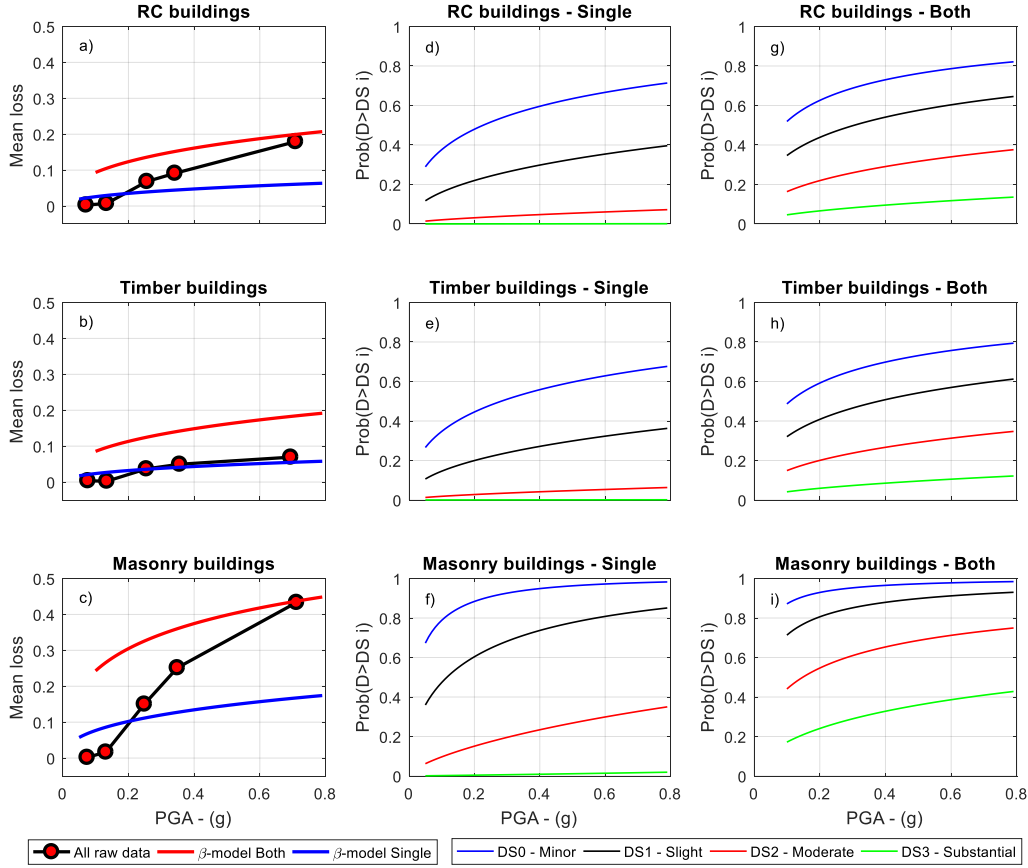


Figure 7. *a,b,c*): Vulnerability functions for RC, timber and masonry buildings for Single and Both events. *d,e,f*): Fragility curves for buildings affected by a Single event, and *g,h,i*): by Both events.

5. CONCLUSIONS

This paper describes a new earthquake vulnerability methodology which can be used to construct statistical vulnerability models in areas affected by sequential earthquake events and where the variability in the loss data is high. The proposed methodology adopts a one parameter adaptive grid approach to aggregate the loss data and another one parameter model to distinguish between buildings affected by a single event or two events. The methodology was applied to a detailed building-by-building and complete loss database which was recorded in the aftermath of the two Mw6.5 South Iceland earthquakes in June 2000. The database covers almost 5,000 low-rise residential buildings constructed by RC, timber or masonry. The losses in the database include both structural and non-structural losses, though excluding losses from household contents. Both vulnerability functions as well as fragility functions are presented for buildings affected by “Single” event and by “Both” events. Despite the fact that many buildings were located near the fault rupture they survived the seismic loads quite well and the probability of getting more than 50% loss (exceeding DS3) was less than 15% for both RC and timber buildings but up to 45% for masonry buildings.

6. ACKNOWLEDGMENTS

The authors wish to offer their thanks to the Icelandic Catastrophe Insurance for placing the earthquake loss database and other relevant information at their disposal, and the University of Iceland for a research grant. Ioanna Ioannou and Tiziana Rossetto's contribution to this study was funded by the HORIZON2020 project 'IMPROVER' (grant number: 653390).

7. REFERENCES

- Akaike H (2011). Akaike's Information Criterion, In: Lovric M, ed. *International Encyclopedia of Statistical Science*, Berlin, Heidelberg: Springer Berlin Heidelberg, 25-25.
- Ambraseys N, Smit P, Sigbjörnsson R, Suhadolc P, Margaris B (2002). Internet-Site for European Strong-Motion Data (ISESD). European Commission.
- Bessason B, Bjarnason JÖ (2016). Seismic vulnerability of low-rise residential buildings based on damage data from three earthquakes (Mw6.5, 6.5 and 6.3), *Engineering Structures*, 111:64-79.
- Bessason B, Bjarnason JÖ, Gudmundsson A, Sólnes J, Steedman S (2012). Probabilistic Earthquake Damage Curves for Low-Rise Buildings Based on Field Data, *Earthquake Spectra*, 28(4):1353-1378.
- Bessason B, Bjarnason JÖ, Guðmundsson A, Sólnes J, Steedman S (2014). Analysis of damage data of low-rise buildings subjected to a shallow Mw6.3 earthquake, *Soil Dynamics and Earthquake Engineering*, 66:89-101.
- Bessason B, Kaynia AM (2002). Site amplification in lava rock on soft sediments, *Soil Dynamics and Earthquake Engineering*, 22(7):525-540.
- D' Ayala D, Meslem A (2013). *Guidelines for analytical vulnerability assessment* Pavia, Italy: GEM Foundation.
- Einarsson P (1991). Earthquakes and present-day tectonism in Iceland, *Tectonophysics*, 189(1):261-279.
- Halldórsson P, Björnsson S, Brandsdóttir B, Sólnes J, Stefánsson R, Bessason B (2013). Earthquakes in Iceland. In: Sólnes J, Sigmundsson F, Bessason B (editors), *Natural Hazard in Iceland, Volcanic Eruptions and Earthquakes*, University of Iceland Press and Iceland Catastrophe Insurance (in Icelandic).
- Icelandic Property Registers. <http://www.skra.is/english/property-register/>. Accessed 10/08, 2017.
- Iceland Catastrophe Insurance. <http://www.vidlagatrygging.is/en/>. Accessed 10/08, 2017.
- Ioannou I, Bessason B, Kosmidis I, Bjarnason JÖ, Rossetto T (2018), Empirical seismic vulnerability assessment of Icelandic buildings affected by the 2000 sequence of earthquakes, Submitted to: *Bulletin of Earthquake Engineering* (Submitted in Sept 2017).
- Jóhannesson H, Jakobsson SP, Sæmundsson K (1982). *Geological map of Iceland, sheet 6, S-Iceland*, Icelandic Museum of Natural history and Iceland Geodetic Survey, Reykjavik, Iceland.
- Neocleous T, Aitken C, Zadora G (2011). Transformations for compositional data with zeros with an application to forensic evidence evaluation, *Chemometrics and Intelligent Laboratory Systems*, 109(1):77-85
- Ólafsson S (2013). Attenuation of earthquake waves. In: Sólnes J, Sigmundsson F, Bessason B (editors). *Natural Hazard in Iceland, Volcanic Eruptions and Earthquakes*: University of Iceland Press and Iceland Catastrophe Insurance, (in Icelandic).
- Park YJ, Ang AH-S (1984). Mechanistic seismic damage model for reinforced concrete, *Journal of Structural Engineering, ASCE*, 111(ST4):722-739.
- Rossetto T, Ioannou I, Grant DN, Maqsood T (2014). *Guidelines for empirical vulnerability assessment*, Pavia, Italy, GEM Foundation.
- Rossetto T, Ioannou I, Grant DN (2013). *Existing empirical fragility and vulnerability relationships: Compendium and guide for selection* Pavia, Italy: GEM Foundation.
- Rupakhety R, Sigbjörnsson R (2009). Ground-motion prediction equations (GMPEs) for inelastic response and structural behaviour factors, *Bulletin of Earthquake Engineering*, 7(3):637-659
- Sigbjörnsson R, Rupakhety R (2014). A saga of the 1896 South Iceland earthquake sequence: magnitudes, macroseismic effects and damage, *Bulletin of Earthquake Engineering*, 12(1):171-184.

Sigbjörnsson R, Snæbjörnsson JT, Higgins SM, Halldórsson B, Ólafsson S (2009). A note on the Mw6.3 earthquake in Iceland on 29 May 2008 at 15:45 UTC. *Bulletin of Earthquake Engineering*.7(1):113-126.

Thórarinnsson Ó, Bessason B, Snæbjörnsson J, Ólafsson S, Sigbjörnsson R, Baldvinsson G (2002). The South Iceland earthquakes 2000: Strong motion measurements. *Proceedings of the 12th European Conference on Earthquake Engineering*, Paris, France, Paper no. 321.

Vogfjord K, Sigbjörnsson R, Snæbjörnsson TTh, Halldórsson B, Sólnes J, Stefánsson R (2013). The South Iceland earthquakes 2000 and 2008, In: Sólnes J, Sigmundsson F, Bessason B (editors), *Natural Hazard in Iceland, Volcanic Eruptions and Earthquakes*, University of Iceland Press and Iceland Catastrophe Insurance (in Icelandic).